Appl. Chem. Eng., Vol. 35, No. 4, August 2024, 346-351
https://doi.org/10.14478/ace.2024.1026

Article

Design of Experiments for Enhanced Catalytic Activity: Cu-Embedded Covalent Organic Frameworks in 4-Nitrophenol Reduction

Sangmin Lee and Kye Sang Yoo †

Department of Chemical & Biomolecular Engineering, Seoul National University of Science and Technology, Seoul 01811, Korea
(Received May 1, 2024; Revised June 1, 2024; Accepted June 1, 2024)

Abstract

Chemical reduction using catalysts and $NaBH_4$ presents a promising approach for reducing 4-nitrophenol contamination while generating valuable byproducts. Covalent organic frameworks (COFs) emerge as a versatile platform for supporting catalysts due to their unique properties, such as high surface area and tunable pore structures. This study employs design of experiments (DOE) to systematically optimize the synthesis of Cu embedded COF (Cu/COF) catalysts for the reduction of 4-nitrophenol. Through a series of experimental designs, including definitive screening, mixture method, and central composition design, the main synthesis parameters influencing Cu/COF formation are identified and optimized: MEL:TPA:DMSO = 0.31:0.36:0.33. Furthermore, the optimal synthesis temperature and time were predicted to be 195 °C and 14.7 h. Statistical analyses reveal significant factors affecting Cu/COF synthesis, facilitating the development of tailored nanostructures with enhanced catalytic performance. The catalytic efficacy of the optimized Cu/COF materials is evaluated in the reduction of 4-nitrophenol, demonstrating promising results in line with the predictions from DOE.

Keywords: *Statistical design of experiments, Covalent organic frameworks, 4-Nitrophenol reduction*

1. Introduction

4-Nitrophenol is widely utilized in diverse industrial domains, including leather, dyestuff, papermaking, medicine, pesticides, printing, textiles, and explosives[1,2]. The presence of nitrophenol in wastewater primarily stems from industrial discharges, agricultural runoff, and microbial breakdown. Its considerable toxicity, solubility in water, stability, and resistance to degradation pose notable environmental and health risks[3]. Of particular concern is its heightened toxicity and production compared to other nitrophenols, prompting regulatory bodies like the USA Environmental Protection Agency (EPA) to prioritize its control. Various methods have emerged to tackle 4-nitrophenol contamination in wastewater, spanning adsorption, extraction, membrane separation, microbial degradation, advanced oxidation, and electrochemical oxidation[4-8]. Chemical reduction of 4-nitrophenol using catalysts and $NaBH_4$ under mild conditions presents a promising method for mitigating environmental hazards while generating valuable aromatic amine byproducts for reuse[9]. Despite their potential, these methods encounter challenges such as high expenses, limited scalability, and complex equipment requirements. Notably, the catalytic reduction of 4-nitrophenol to 4-aminophenol using catalysts and $NaBH_4$ has been extensively explored, employing diverse nanomaterials like precious metal nanoparticles, metal oxides, carbon materials, metal-organic frameworks, and composites[10-12]. However, maintaining the optimal activity and stability of catalysts remains a difficult hindrance. Thus, the design of tailored nanostructures to enhance the catalytic performance may offer a promising strategy for supplementing overall efficiency.

Covalent organic frameworks (COFs) represent a new class of crystalline organic porous polymers, predominantly composed of lightweight elements (C, H, N, O, B, etc.) linked by reversible covalent bonds to form a framework structure[13,14]. These materials typically possess prominent characteristics such as high specific surface area, porosity, stability, and low density in comparison to inorganic nanomaterials[15]. As a result of these exceptional properties, COFs find wide-ranging applications in gas storage and separation, catalysis, photochemical conversion, biomaterials, energy storage and conversion [16-20]. Of particular significance is the ordered pore structures, tunable pore sizes, and substantial specific surface areas exhibited by COFs, rendering them promising carriers for catalytic reactions. For example, COFs have been engineered to support ultrafine Pt or Pd nanoparticles, demonstrating excellent catalytic performance in various reactions. While COFs have displayed potential in supporting catalysts, further exploration is acceptable to realize their multifaceted applications. Therefore, the advancement of COF-supported metal catalysts holds considerable promise in furnishing active sites, enhancing stability, and catalytic activity.

Design of experiments (DOE) is a systematic statistical method used in research and industry to plan, conduct, analyze, and interpret experiments with the aim of maximizing information gain while minimizing the influence of extraneous factors[21-24]. Its primary goal is to identi-

† Corresponding Author: Seoul National University of Science and Technology Department of Chemical & Biomolecular Engineering, Seoul 01811, Korea
Tel: +82-2-970-6602 e-mail: kyoo@seoultech.ac.kr

pISSN: 1225-0112 eISSN: 2288-4505 @ 2024 The Korean Society of Industrial and Engineering Chemistry. All rights reserved.

fy critical factors affecting a process or product and optimize them to achieve desired outcomes. DOE involves intentionally selecting and adjusting specific variables (known as factors) while observing their impact on a response variable, which can be categorical or continuous. Widely applicable across various fields including engineering, manufacturing, pharmaceuticals, agriculture, and social sciences, DOE encompasses different experiment designs such as screening, factorial, and response surface experiments. By employing DOE, researchers gain a comprehensive understanding of the system under study, enabling data-driven executive and facilitating improvements in product quality, process efficiency, and service effectiveness. In this study, DOE methods were employed consecutively to evaluate Cu/COF synthesis processes. Initially, a screening method was used to identify important precursors for the synthesis. Subsequently, a mixture method was applied to optimize the ratios of selected precursors. The amount of CHN elements was used as a response factor to determine Cu/COF properties. Finally, designated Cu/COF samples were evaluated as a catalyst for 4-nitrophenol reduction.

2. Experiments

Distilled water (DIW), ethylenediamine, melamine (MEL), terephthaldehyde (TPA), dimethylsulfoxide (DMSO), and ethanol were obtained from Sigma-Aldrich. Copper nanoparticles were purchased from DS High Metal. All chemicals were used as received without further purification. Copper, melamine, terephthaldehyde, dimethylsulfoxide, and distilled water were stirred for 10 minutes. The quantities of each reagent were adjusted based on concentration ratios determined by design methods. The resulting mixture was then transferred to an autoclave and reacted in an oven at designed temperature and duration. Following the reaction, the final product was obtained through filtration, washed with ethanol, and dried at room temperature, yielding the Cu/COF catalyst. The C, H, N, S elemental analysis of the sample was performed at 950 °C using a Thermo Scientific elemental analyzer (FLASH EA 1112, USA) with sulfamethazine (C: 51.8%, H: 5.1%, N: 20.1%, S: 11.5%) as a standard.

The Cu/COF particles, prepared beforehand, were utilized for catalyzing the reduction of 4-nitrophenol in the presence of $NaBH_4$. In a standard catalytic reaction, a 10 mM aqueous solution of 4-nitrophenol and a 20 mM aqueous solution of $NaBH_4$ underwent the degradation process in the presence of COF-supported nanoparticles. Initially, the color of the mixed solution of 4-nitrophenol and $NaBH_4$ transitioned from a mild yellow to a deeper shade. Subsequently, 10 mg of Cu/COF was introduced into the solution under vigorous stirring. Finally, the catalytic reactions were monitored using UV-Vis absorption spectroscopy within a scanning range of 275~500 nm.

Statistical analyses were performed using Minitab 21 software. The Assistant DOE module within Minitab 21 offers a streamlined sequential experimentation approach, starting with screening designs to identify crucial factors. This is followed by more detailed designs to detect curvature and establish an optimal model for identifying factor settings that optimize the response.

3. Results and discussion

3.1. Definitive screening design

A definitive screening design was utilized to determine the main factors influencing the synthesis of Cu/COF particles. The precursors, TPA, MEL, DMSO, and DIW, were incorporated into the design, with each factor set at three different levels, as detailed in Table 1. Thirteen different Cu/COF samples were designed with varying in precursor concentrations, while maintaining a constant reaction temperature of 180 °C for 12 h. After synthesis of the samples, the amounts of C, H, and N were determined using an element analyzer. The chemical structure of Cu/COF entails a reticular construction comprised of $C_3N_3H_6$ rings from melamine and benzene from terephthalaldehyde, covalently bonded to Cu with N acting as the bridge. Thus, a well-defined COF structure exhibits higher elemental content of C, H, and N. Hence, in subsequent statistical analyses, the amount of C, H, and N were employed as indicators of the Cu/COF structure.

Statistical analysis was conducted to explore the significance of input factors and their interactions with output responses (total amount of C, H, N). Initially, a Pareto chart was generated to assess the importance of the factors, as illustrated in Figure 1. The relative importance and statistical significance among the main factors were observed on the Pareto chart. MEL (A), TPA (B), and DMSO (C) emerged as significant synthesis conditions for Cu/COF samples. To evaluate the impact of the four factors on the C, H, N content (response), main effect plots were depicted in Figure 2. Main effect plots serve to examine the differences in response means among vari-

Table 1. Factors and Levels for Definitive Screening Design

Factor	Level		
	Low	Middle	High
Terephthaldehyde	0.1 g	0.25 g	0.4 g
Melamine	0.1 g	0.25 g	0.4 g
Dimethylsulfoxide	5 mL	12.5 mL	20 mL
Distilled water	1 mL	2.5 mL	4 mL

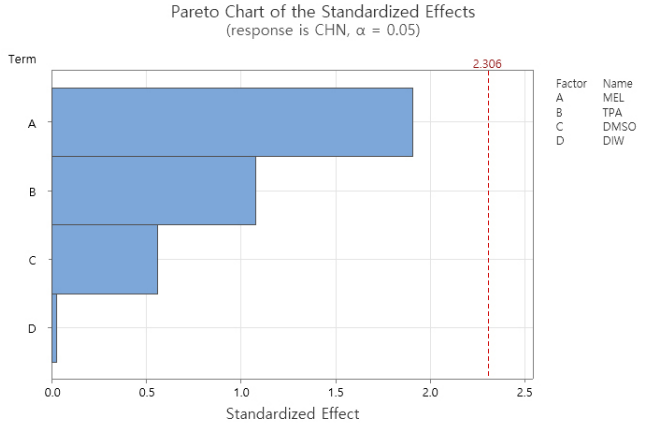

Figure 1. Pareto chart for the effects of precursor of Cu/COF synthesis on CHN amount designed by definitive screening design.

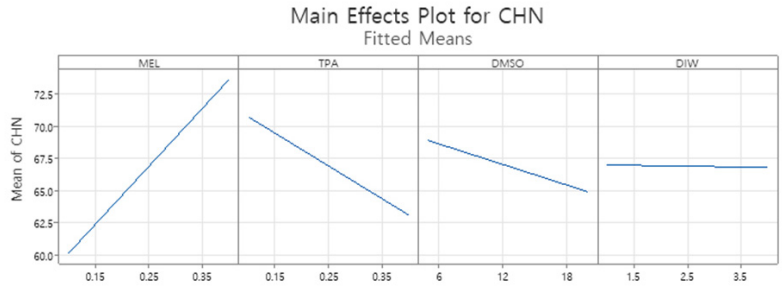

Figure 2. Main effects plot on CHN amount of Cu/COF with various synthesis conditions designed by definitive screening design.

ous levels of a factor and to identify the presence of a main effect when the response is influenced by varying levels of a factor. These plots illustrate the response means for each level of a factor connected by a line. A non-horizontal line indicates the presence of a main effect, with the steepness of the slope indicating the magnitude of the effect. Consequently, the DIW (D) factor could be deemed negligible in optimizing the synthesis reaction conditions.

3.2. Mixture method

The mixture design method was employed to determine the optimal composition of precursors in Cu/COF synthesis. This method represents a specialized form of response surface design tailored for analyzing products composed of multiple components or ingredients. Particularly effective in industrial development scenarios involving formulations or mixtures, this experimental design hinges on the proportions of individual components within the mixture to yield desired outcomes. An extreme vertices design, a methodology within the mixture design, was used in this investigation. This approach introduces additional constraints on the design, as the lower and upper bounds of the proportion of each ingredient are not strictly confined to the conventional 0 to 1 range. Instead, these values are dictated by the molar concentrations of the materials. Specifically, a modified molar ratio was adopted to streamline the design process within the mixture method.

Thirteen compositions of three precursors, MEL, TPA, and DMSO, were designed using Minitab software. Cu/COF samples were then prepared with these predetermined precursor concentrations under identical reaction conditions. Subsequently, the total amounts of C, H, and N were determined as responses. Analysis of variance (ANOVA) was conducted based on these values. Among the values in Table 2, particular attention was given to the p-value, which serves as a measure of the probability that an observed difference could have arisen purely by random chance. A lower p-value (typically less than 0.05) indicates greater statistical significance. In this case, the p-value of the regression analysis was calculated to be 0.009, underscoring the statistical significance of the model. While the p-value of the linear terms of the model was slightly elevated, the overall predictability of the results generated by the mixture design utilized in this study remained highly reliable for further investigation.

The mixture contour plot depicting the CHN amount of Cu/COF samples synthesized with various molar fractions of precursors is illustrated in Figure 3. A region featuring the maximum CHN amount was

Table 2. Analysis of Variance (ANOVA) for Mixture Design

Source	DF	Seq SS	Adj SS	Adj MS	F-value	P-value
Regression	5	1504.77	1504.8	300.95	7.67	0.009
Linear	2	133.09	237.9	118.94	3.03	0.113
Square	3	1371.68	1371.7	457.23	11.66	0.004
MEL × TPA	1	0.46	265.6	265.62	6.77	0.035
MEL × DMSO	1	153.39	628.9	628.94	16.03	0.005
TPA × DMSO	1	1217.83	1217.8	1217.83	31.04	0.001
Error	7	274.61	274.6	39.23		
Total	12	1779.38				

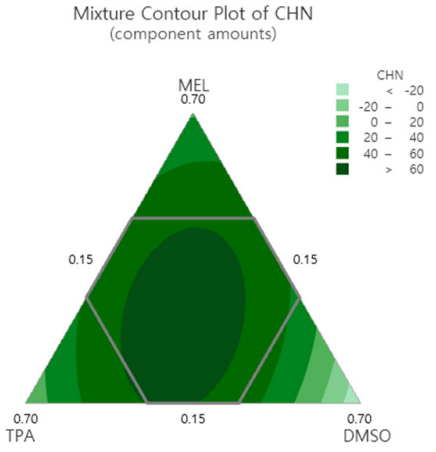

Figure 3. Mixture contour plot of CHN amount of Cu/COF synthesized with various mole fractions of precursors.

predicted to be situated at the lower center of the triangle, with a rapid decrease in response observed towards the vertices of the triangle. The Cox response trace plot as shown in Figure 4, elucidates the effects of altering each mixture component while maintaining all others at a constant ratio. The trace curves delineate the impact of modifying the corresponding component along an imaginary line (direction) connecting the reference blend to a vertex. This plot aids in identifying the most influential components, which can then be mapped onto a contour or surface plot. This observation aligns well with the trends previously discussed. Furthermore, the presence of an optimal composition was detected for all three components. The optimal molar ratio of the three precursors for Cu/COF synthesis was identified using the response op-

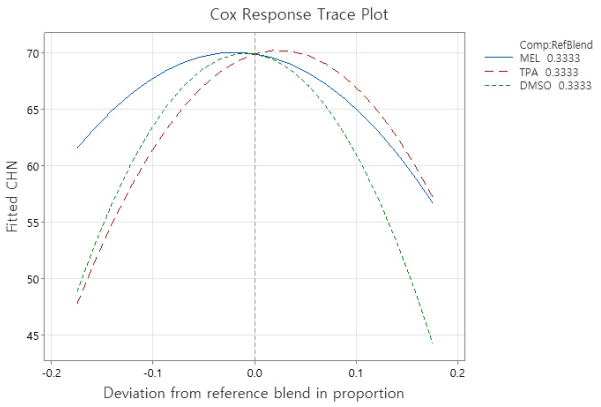

Figure 4. Cox response trace plot of CHN amount of Cu/COF based on precursor composition.

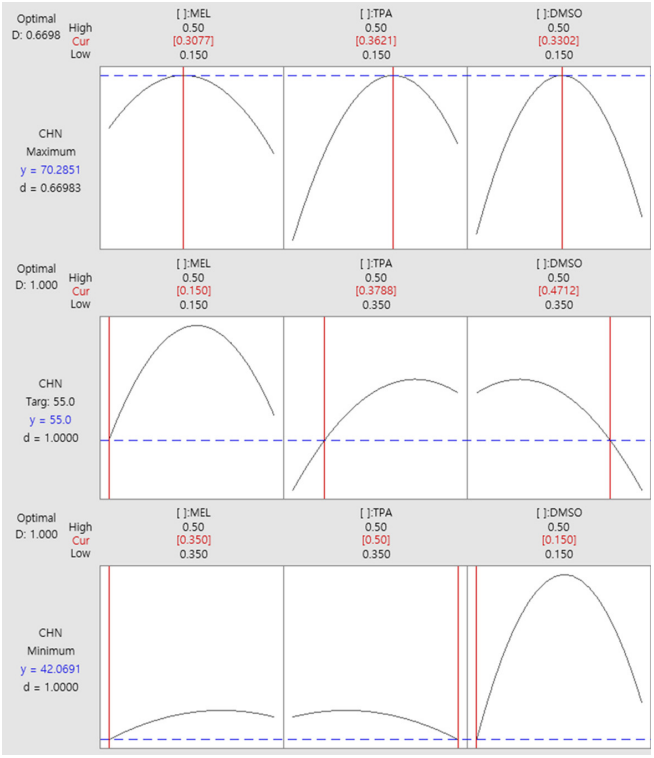

Figure 5. The optimized responses for Cu/COF samples synthesized with various mole fractions of precursors, targeting maximum (S1), median (S2), and minimum (S3) levels of CHN amount.

timizer tool, which elucidates how various experimental settings influence the predicted responses for a stored model. The molar ratios for Cu/COF synthesis to achieve maximum, median, and minimum level of CHN amounts were predicted, as illustrated in Figure 5. Subsequently, three Cu/COF samples were synthesized at these calculated ratios determined by the optimizer and utilized for catalytic activity measurements.

3.3. Central composition design

The significant factors influencing Cu/COF synthesis, particularly the CHN amounts, were identified in the preceding section. To further

Table 3. Factors and Levels for Central Composition Design

Factor	Level				
	$-\alpha$	-1	0	+1	$+\alpha$
Temp. (°C)	140	160	180	200	220
Time (h)	6	8	12	16	18

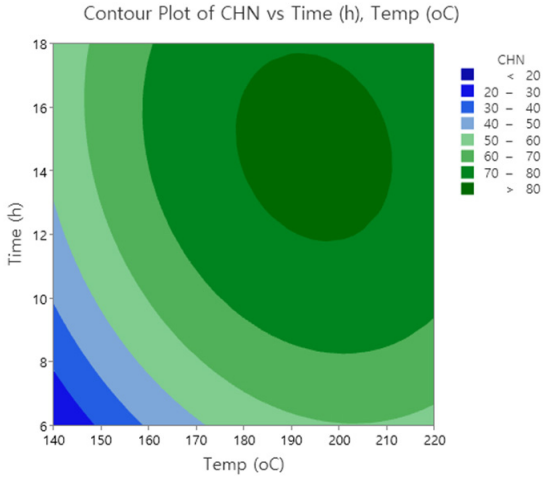

Figure 6. Contour plot for CHN amount of Cu/COF synthesized with various synthesis conditions designed by central composition design.

optimize these factors, the response surface method (RSM) was employed, providing a suite of advanced design of experiment techniques for enhanced understanding and optimization of responses. RSM serves to refine models subsequent to determining significant factors using prior design methods. Leveraging a quadratic regression model, RSM aids in comprehending or mapping regions of a response surface, determining variable levels to optimize a response, and selecting operational conditions to meet specifications. In this study, the central composite design (CCD), one of RSM methods, was practically implemented. CCD is capable of fitting a full quadratic model by incorporating information from a well-planned factorial experiment.

Experiments were planned with the CCD method to optimize two primary factors: synthesis temperature and time. The factors and their corresponding levels for the design are outlined in Table 3. Nine experimental runs were proposed, and elemental analyses were conducted accordingly. The synthesis temperature and time were varied while keeping the concentration ratio of the precursor that exhibited the maximum level of CHN amount. The results of fitting the quadratic response surface model, as evidenced by analysis of ANOVA, are presented in Table 4. ANOVA dissects the overall variation of the results into segments associated with the model and those linked to experimental errors, indicating whether the variance from the model is statistically significant. This assessment was facilitated by the P-value, which serves as a reliable predictor of the experimental data. The obtained P-value in this analysis was 0.000, signifying the validity of the model.

Figure 6 displays a contour plot illustrating the CHN amount of Cu/COF synthesized across various temperature and time settings. A

Table 4. Analysis of Variance (ANOVA) for Central Composition Design

Source	DF	Adj SS	Adj MS	F-value	P-value
Model	5	1585.22	317.044	77.44	0.000
Linear	2	431.84	215.922	52.74	0.000
Temp.	1	429.91	429.913	105.01	0.000
Time	1	107.12	107.117	26.16	0.001
Square	2	457.57	228.783	55.88	0.000
Temp. × Temp.	1	372.32	372.318	90.94	0.000
Time × Time	1	195.61	195.615	47.78	0.000
2-way interactions	1	9.61	9.610	2.35	0.169
Temp. × Time	1	9.61	9.610	2.35	0.169
Error	7	28.66	4.094		
Lack of fit	3	26.59	8.864	17.14	0.010
Pure error	4	2.07	0.517		
Total	12	1613.88			

contour plot offers a two-dimensional perspective wherein contours connect points with equal response values. As both synthesis temperature and time increased, CHN amounts of the samples improved, as evidenced in the contour plot. Notably, synthesis conditions yielding the highest value were clearly discernible in the plot. To further refine the synthesis conditions, the response optimizer tool was utilized to investigate how different experimental settings impact the predicted responses based on a stored model. According to the analysis, Cu/COF synthesized at 195 °C for 14.7 h was calculated to exhibit the maximum amount of CHN elements.

3.4. 4-nitrophenol reduction

The catalytic performance of Cu/COF materials was explored through the reduction of 4-nitrophenol (4-NP) to 4-aminophenol (4-AP) using $NaBH_4$ at ambient temperature. Investigation of the reduction process was facilitated by UV−Vis absorption spectroscopy. Initially, the characteristic absorption peak at 317 nm indicated the presence of 4-NP in the aqueous solution. Upon introducing the catalyst into the mixture, a new absorption peak emerged near 300 nm, corresponding to 4-AP. Simultaneously, the original absorption peak of 4-NP at 400 nm vanished, suggesting the successful catalytic conversion to 4-AP. The catalytic reduction followed the Langmuir-Hinshelwood apparent first-order kinetics model. Given the substantial excess of $NaBH_4$ compared to 4-NP concentration, the reaction was assumed to be first-order, independent of $NaBH_4$ concentration. The catalytic reduction proceeded according to pseudo-primary kinetics, with an apparent reaction rate constant. The catalytic performance evaluation of the three materials selected using DOE was performed under the identical conditions. Three samples derived in Figure 5, the materials synthesized under the conditions with the maximum (S1), medium (S2), and minimum (S3) values based on the total amount of CNH, were used as catalysts. The results of comparing the reaction rate constant calculated from the catalytic experiment with the total amount of CNH are shown in Figure 7. As a result, a similar trend of both values was observed. This indicates that the catalytic performance predicted by the statistical design of experiments and the actual experimental values are meaningful.

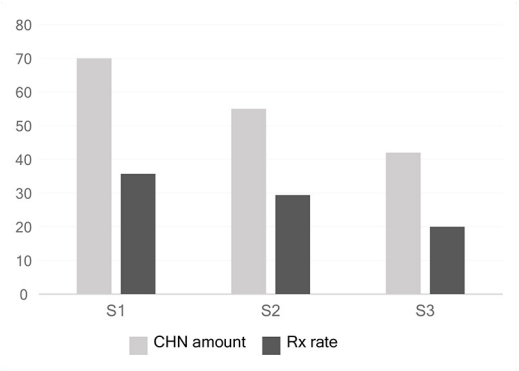

Figure 7. Catalytic performance of the Cu/COF materials with various precursor compositions for the reduction of 4-nitrophenol.

4. Conclusion

In conclusion, a comprehensive investigation employing various experimental design methodologies was conducted to optimize the synthesis of Cu/COF particles and evaluate their catalytic performance in 4-nitrophenol reduction. The definitive screening design initially identified significant synthesis factors, MEL, TPA, and DMSO, while indicating the negligible impact of DIW. Subsequently, the mixture method allowed for precise determination of precursor composition, unveiling an optimal molar ratio for Cu/COF synthesis. Leveraging the response surface method through central composite design further refined synthesis conditions, with synthesis temperature and time pinpointed as key factors influencing Cu/COF synthesis. The successful reduction of 4-nitrophenol to 4-aminophenol using Cu/COF catalysts validated the efficacy of the optimized synthesis parameters. The congruence between predicted catalytic performance and experimental results underscores the significance and reliability of the statistical design

of experiments in materials synthesis and catalysis research. This systematic approach not only enhances our understanding of Cu/COF synthesis but also offers a robust framework for optimizing the performance of other catalytic materials in diverse applications.

Acknowledgment

This study was supported by the Research Program funded by the SeoulTech(Seoul National University of Science and Technology)

References

1. B. K. Ghosh, S. Hazra, B. Naik, and N. N. Ghosh, Preparation of Cu nanoparticle loaded SBA-15 and their excellent catalytic activity in reduction of variety of dyes, *Powder Technol.*, **269**, 371-378 (2015).
2. H. Lu, H. Yin, Y. Liu, T. Jiang, and L. Yu, Influence of support on catalytic activity of Ni catalysts in p-nitrophenol hydrogenation to p-aminophenol, *Catal. Commun.*, **10**, 313-316 (2008).
3. G. Eichenbaum, M. Johnson, D. Kirkland, P. O'Neill, S. Stellar, J. Bielawne, R. DeWire, D. Areia, S. Bryant, S. Weiner, D. Desai-Krieger, P. Guzzie-Peck, D. C. Evans, and A. Tonelli, Assessment of the genotoxic and carcinogenic risks of pnitrophenol when it is present as an impurity in a drug product, *Regul. Toxicol. Pharmacol.,* **55**, 33-42 (2009).
4. P. T. Huong, B. K. Lee, J. Kim, and C. H. Lee, Nitrophenols removal from aqueous medium using Fe-nano mesoporous zeolite, *Mater. Des.*, **101**, 210-217 (2016).
5. B. Cui, J. C. Gong, M. H. Duan, Z. X. Chang, L. L. Su, W. J. Liu, and D. L. Li, Reactive extraction of *p*-nitrophenol using tributylphosphate in solvent naphtha or *n*-octanol, *J. Chem. Eng. Data*, **61**, 813-819 (2016).
6. S. Chaouchi and O. Hamdaoui, Removal of 4-nitrophenol from water by emulsion liquid membrane, *Desalin. Water Treat.*, **57**, 5253-5257 (2016).
7. C. Nie, N. Shao, B. Wang, D. Yuan, X. Sui, and H. Wu, Fully solar-driven thermo- and electrochemistry for advanced oxidation processes (STEP-AOPs) of 2-nitrophenol wastewater, *Chemosphere*, **154**, 604-612 (2016).
8. G. Fadillah, T. A. Saleh, and S. Wahyuningsih, Enhanced electrochemical degradation of 4-nitrophenol molecules using novel Ti/TiO_2-NiO electrodes, *J. Mol. Liq.*, **289**, 111108 (2019).
9. P. Zhao, X. Feng, D. Huang, G. Yang, and D. Astruc, Basic concepts and recent advances in nitrophenol reduction by gold- and other transition metal nanoparticles, *Coord. Chem. Rev.*, **287**, 114-136 (2015).
10. M. Zhang, X. Su, L. Ma, A. Khan, L. Wang, J. Wang, A. S. Maloletnev, and C. Yang, Promotion effects of halloysite nanotubes on catalytic activity of Co_3O_4 nanoparticles toward reduction of 4-nitrophenol and organic dyes, *J. Hazard. Mater.*, **403**, 123870 (2021).
11. J. Li, F. Wu, L. Lin, Y. Guo, H. Liu, and X. Zhang, Flow fabrication of a highly efficient Pd/UiO-66-NH_2 film capillary microreactor for 4-nitrophenol reduction, *Chem. Eng. J.*, **333**, 146-152 (2018).
12. C. Gao, L. Xiao, J. Zhou, H. Wang, S. Zhai, and Q. An, Immobilization of nanosilver onto glycine modified lignin hydrogel composites for highly efficient p-nitrophenol hydrogenation, *Chem. Eng. J.*, **403**, 126370 (2021).
13. C. S. Diercks and O. M. Yaghi, The atom, the molecule, and the covalent organic framework, *Science*, **355**, eaal1585 (2017).
14. S. Y. Ding and W. Wang, Covalent organic frameworks (COFs): from design to applications, *Chem. Soc. Rev.*, **42**, 548-568 (2013).
15. S. Das, P. Heasman, T. Ben, and S. Qiu, Porous organic materials: Strategic design and structure−function correlation, *Chem. Rev.*, **117**, 1515-1563 (2017).
16. M. X. Wu and Y. W. Yang, Applications of covalent organic frameworks (COFs): From gas storage and separation to drug delivery, *Chin. Chem. Lett.*, **28**, 1135-1143 (2017).
17. J. Tang, C. Su, and Z. Shao, Covalent organic framework (COF)-based hybrids for electrocatalysis: Recent advances and perspectives, *Small Methods*, 5, 2100945 (2021).
18. H. Wang, H. Wang, Z. Wang, L. Tang, G. Zeng, P. Xu, M. Chen, T. Xiong, C. Zhou, X. Li, D. Huang, Y. Zhu, Z. Wang, and J. Tang, Covalent organic framework photocatalysts: Structures and applications, *Chem. Soc. Rev.*, **49**, 4135-4165 (2020).
19. S. Bhunia, K. A. Deo, and A. K. Gaharwar, 2D Covalent organic frameworks for biomedical applications, *Adv. Funct. Mater.*, **30**, 2002046 (2020).
20. J. Li, X. Jing, Q. Li, S. Li, X. Gao, X. Feng, and B. Wang, Bulk COFs and COF nanosheets for electrochemical energy storage and conversion, *Chem. Soc. Rev.*, **49**, 3565-3604 (2020).
21. S. Bisgaard, Industrial use of statistically designed experiments: Case study references and some historical anecdotes, *Quality Eng.*, **4**, 547-562 (1992).
22. M. A. Sedghamiz, S. Raeissi, F. Attar, M. Salimi, and K. Mehrabi, In-situ transesterification of residual vegetable oil in spent bleaching clay with alkali catalysts using CCD-RSM design of experiment, *Fuel*, **237**, 515-521 (2019).
23. Y. Seki, S. Seyhan, and M. Yurdakoc, Removal of boron from aqueous solution by adsorption on Al_2O_3 based materials using full factorial design, *J. Hazard. Mater.*, **138**, 60-66 (2006).
24. L. Ilzarbe, M. J. Alvarez, E. Viles, and M. Tanco, Practical applications of design of experiments in the field of engineering: A bibliographical review, *Qual. Reliab. Eng. Int.*, **24**, 417-428 (2008).

Authors

Sangmin Lee; M.Sc., Graduate Student, Department of Chemical & Biomolecular Engineering, Seoul National University of Science & Technology, Seoul 01811, Korea; leesangmin0529@dsmetal.com

Kye Sang Yoo; Ph.D., Professor, Department of Chemical & Biomolecular Engineering, Seoul National University of Science & Technology, Seoul 01811, Korea; kyoo@seoultech.ac.kr